Journal of Solid State Chemistry 226 (2015) 101–106

Contents lists available at ScienceDirect

Journal of Solid State Chemistry

journal homepage: www.elsevier.com/locate/jssc

Phase transformations during H*Ln*TiO$_4$ (*Ln*=La, Nd) thermolysis and photocatalytic activity of obtained compounds

Oleg I. Silyukov*, Liliia D. Abdulaeva, Alena A. Burovikhina, Ivan A. Rodionov, Irina A. Zvereva

Institute of Chemistry, Saint Petersburg State University, Universitetsky Pr. 26, Saint Petersburg 198504, Russia

ARTICLE INFO

Article history:
Received 11 November 2014
Received in revised form
16 January 2015
Accepted 9 February 2015
Available online 19 February 2015

Keywords:
Layered perovskite-like oxides
Solid state reactions
Phase transitions
Photocatalytic activity

ABSTRACT

Layered H*Ln*TiO$_4$ (*Ln*=La, Nd) compounds belonging to Ruddlesden–Popper phases were found to form partially hydrated compounds $Ln_2Ti_2O_7 \cdot xH_2O$ during thermal dehydration as well as defect oxides $Ln_2{\square}Ti_2O_7$ as final products. Further heating of metastable defect $Ln_2{\square}Ti_2O_7$ substances leads to the formation of pyrochlore-type oxides $Ln_2Ti_2O_{7\ (p)}$, with subsequent transformation under higher temperatures to stable layered 110-type perovskites $Ln_2Ti_2O_7$. The occurring structure transformations lead to an increase of photocatalytic activity in the order of H*Ln*TiO$_4$ < $Ln_2Ti_2O_7 \cdot yH_2O$ < $Ln_2{\square}Ti_2O_7$ < $Ln_2Ti_2O_{7\ (p)}$ < $Ln_2Ti_2O_7$ in the reaction of hydrogen evolution from aqueous isopropanol solution.

1. Introduction

Layered perovskite-like oxides are solid crystalline substances formed by two-dimensional nanosized perovskite slabs interleaved with cations or cationic structural units. Until present time perovskite-like compounds are actively studied as materials with wide range of important physical and chemical properties, such as super-conductivity [1], colossal magnetoresistance [2], ferroelectricity [3,4], catalytic and photocatalytic activity [5–7], thermochemical properties [8] and electrochemical properties [9]. In recent years, there has been a constant interest in using the soft chemistry methods for development of new layered perovskite-like compounds with specified physicochemical properties, as well as design of these materials based on perovskite structure [10–14].

Protonic forms of transition metal layered perovskite-like oxides can be synthesized from alkali compounds, initially prepared by high temperature solid state reaction, during the ion-exchange reaction with acid [15] or by protonation in water [16,17]. They attract great attention due to their interesting and variable properties, in particular the proton conductivity [18,19]. From the other side, such protonated compounds are interesting in terms of their application as precursors for low-temperature reactions and as starting compounds for building nanostructured materials. Ion-exchange reactions of interlayer protons [20], intercalation and exfoliation reactions [21,22], topochemical dehydration are the most important soft chemistry routes for this aim [11].

The possibility of metastable structure formation as the result of protonated layered compounds dehydration was described earlier for different substances. For example, a new form of TiO_2 (B) was obtained from $H_2Ti_8O_{17}$ [23,24], $H_2Ti_3O_7$ and $H_2Ti_5O_{11}$ [25]. Dehydrated layered perovskites and the three-dimensional perovskites with general formula $Ln_2Ti_3O_9$ can be obtained from $H_2Ln_2Ti_3O_{10}$ [26–28], as well as the defective layered perovskite-type oxides $Ln_2{\square}Ti_2O_7$ from H*Ln*TiO$_4$ [15,29].

In the present work the phase transitions during the thermolysis process of protonated H*Ln*TiO$_4$ (*Ln*=La, Nd) related to the Ruddlesden–Popper perovskite-type phases were studied in order to investigate intermediate stages of metastable $Ln_2{\square}Ti_2O_7$ oxides formation and their further evolution to stable compounds. Photocatalytic activity of initial, intermediate and final compounds was measured in order to demonstrate how the occurring topotactic phase transformations affect the physic-chemical properties of compounds under investigation.

2. Experimental

Layered oxides Na*Ln*TiO$_4$ (*Ln*=La, Nd) were prepared by conventional solid state reaction in air at atmospheric pressure using Na_2CO_3, La_2O_3, Nd_2O_3 and TiO_2 as reagents (99.9%, Vecton). The stoichiometric amounts of oxides with 40% excess of sodium

* Correspondence to: Universitetskiy Prospect, 26, Petrodvoretz 198504, Saint-Petersburg, Russia. Tel.: +7 812 4284051.
E-mail address: olegsilyukov@yandex.ru (O.I. Silyukov).

http://dx.doi.org/10.1016/j.jssc.2015.02.008
0022-4596/

carbonate were ground in agate mortar, pelletized by pressure and heated in a corundum crucible. Calcination was carried out at 780 °C for 2 h and then continued at 900 °C for 3 h in air according to results of the formation and thermal stability investigation of $NaNdTiO_4$ [30,31]. The protonated forms $HLnTiO_4$ were prepared from $NaLnTiO_4$ by ion exchange reaction with a three-fold excess of 0.1 M HCl. For this purpose initial Na-containing oxides were ground, suspended in HCl solution, and stirred at 25 °C during 48 h. The as-prepared H-containing phases were centrifuged, washed with distilled water and dried at room temperature over CaO.

The investigation of the dehydration processes was performed by means of thermogravimetric analysis (TG 209 F1 Libra, Netzsch) and simultaneous thermal analysis (TG and DSC) (STA 449 F1 Jupiter, Netzsch) coupled with quardrupole mass spectrometer QMS 403C Aëolos. TG studies were performed in the flow of argon and dried air (90 mL/min) at a heating rate of 10 °C/min. STA studies were performed in the flow of argon (70 mL/min) at a heating rate of 20 °C/min. XRD analysis data were collected with Rigaku MiniFlex II diffractometer (powder X-ray diffraction, Cu$K\alpha$ radiation). Thermo XRD data (powder X-ray diffraction, Cu$K\alpha$ radiation) during thermolysis process were collected with Rigaku Ultima IV diffractometer with heating rate of 10 °C/min, and 2 min preheating before XRD data collection, scanning step 50 °C, scanning range 50–1000 °C. Scanning electron microscopy (SEM) was performed on a Zeiss Merlin scanning electron microscope. IR spectra of the samples were recorded with a FT-IR spectrometer IRPrestige-21, using the KBr pellet technique. Photocatalytic activity in the reaction of hydrogen evolution from aqueous isopropanol solution was measured on a custom designed set-up described in previous papers [6,32]. The reaction suspension composed of 60 mg oxide sample and 60 mL 0.1 (mol%) isopropyl alcohol aqueous solution was shaken and left for a day to establish adsorption equilibrium. Immediately before the experiment, each suspension was sonicated for 10 min (Elmasonic S10H ultrasound bath) to disaggregate the oxide particles and then was placed into an external-irradiation photocatalytic reaction cell, equipped with a magnetic stirrer and connected to a closed gas circulation system. A medium-pressure mercury lamp DRT-125 (125W) was used as a radiation source. A light filter solution (KCl + NaBr, each 6 g/L) thermostated at 15 °C was used to cut off radiation with $\lambda < 220$ nm. At the beginning of each experiment, the suspension was saturated with argon gas to remove air from the system. Hydrogen evolved during the photocatalytic reaction accumulates in the gas phase of 125 ml total volume, which initially contains argon at atmospheric pressure. The gas composition was analyzed by an on-line gas chromatograph (Shimadzu GC-2014, TCD, Msieve 5A Column). The photocatalytic reaction rate was calculated from the slope of the hydrogen evolution kinetic curves.

3. Results and discussion

3.1. Simultaneous thermal analysis studies

STA (TG and DSC) coupled with QMS shows the thermal behavior of $HLnTiO_4$ compounds. The dehydration process was found to be quite complex (Fig. 1).

The first stage from the beginning of heating (Table 1, step 1) is surface water evaporation with 0.23% weight loss for $HNdTiO_4$ and more than 0.71% for $HLaTiO_4$ which is more hygroscopic like most La-containing compounds. After that four main thermal effects are presented. Thermal decomposition starts with the exothermic effect accompanied with only small weight loss (Table 1, step 2) suggesting that a phase transition takes place. During further heating the major weight loss occurs for both compounds with small endothermic effect (Table 1, step 3). Despite the fact that weight loss due to release of water is usually accompanied by endothermic heat effect in that case it could be compensated by exothermic effect related to the formation of defective layered perovskite structure. After that DSC detects two more exothermic processes, first of them under lower temperatures (Table 1, step 4) and the second under high temperature (Table 1, step 5), without any significant weight loss suggesting that two more phase transitions are expected.

TG and DSC were supplemented by mass-spectrometry data, which shows that ion current (IC), detected during heating, corresponds to the elimination of water molecules (Fig. 1), without CO_2, HCl or other possible impurities.

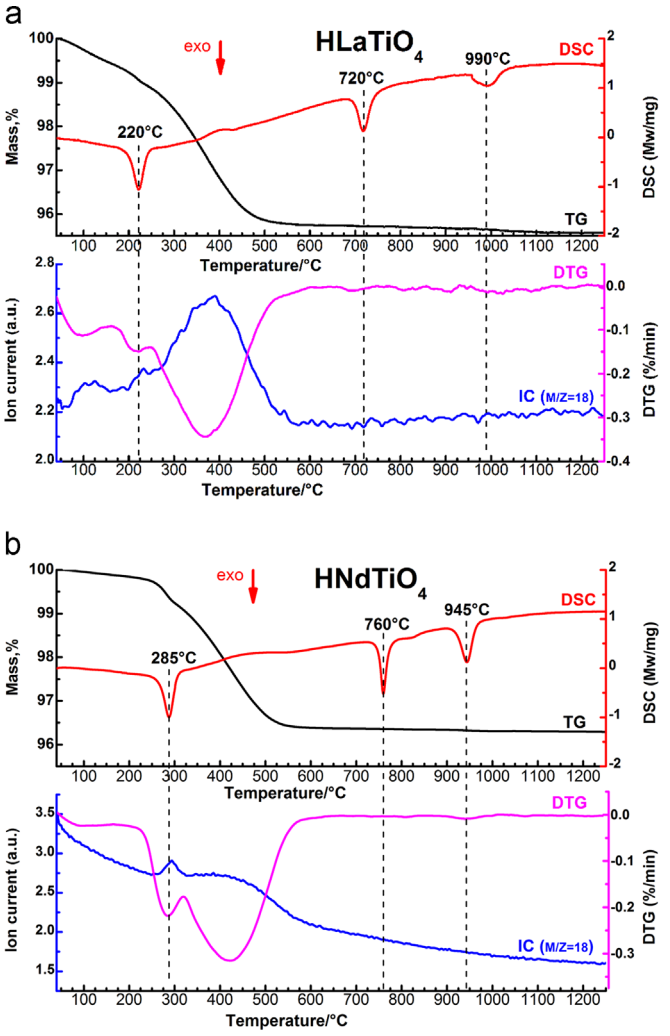

Fig. 1. STA results for (a) $HLaTiO_4$ and (b) $HNdTiO_4$, TG and DSC data (top), DTG and ion current (IC) data (bottom).

Table 1
TG and DSC data of $HLaTiO_4$ and $HNdTiO_4$.

Sample	$HLaTiO_4$				$HNdTiO_4$			
	T_{onset} (°C)	T_{endset} (°C)	Δm (%)	ΔH (kJ/mol)	T_{onset} (°C)	T_{endset} (°C)	Δm (%)	ΔH (kJ/mol)
Step 1	30	160	0.71	n/a	30	235	0.23	n/a
Step 2	160	250	1.08	−15.5	235	305	0.76	−16.4
Step 3	250	600	2.4	n/a	305	625	2.65	n/a
Step 4	675	765	–	−18.7	720	795	–	−14.5
Step 5	965	1065	–	−11.7	915	990	–	−18.6

3.2. Powder X-ray diffraction studies

Comparison of STA results with thermo-XRD data (Fig. 2) shows that structural transformations begin after the first exothermic stage of H*Ln*TiO_4 dehydration (220 °C for La and 285 °C for Nd).

As it can be seen from TG (Fig. 1), H*Ln*TiO_4 samples calcined at 500 °C should be fully dehydrated, while heating up to 150 °C leads only to surface water elimination. In the temperature range from 150–200 °C to 450–500 °C oxides $Ln_2Ti_2O_7 \cdot xH_2O$ with different remaining water content exist.

We also performed discrete step TG with the same temperature program as Thermo XRD (provided in Supplementary information) to properly connect the STA and Thermo XRD data. Accordingly, XRD patterns at temperatures before full water elimination were recorded during the dehydration process, thus peaks at higher angles correspond to the intermediate compounds with lower water content than peaks at lower angles. Anyway the shift of the first peak to the higher angles with temperature increasing corresponds to the decrease of *c* lattice parameter of corresponding compounds during the dehydration.

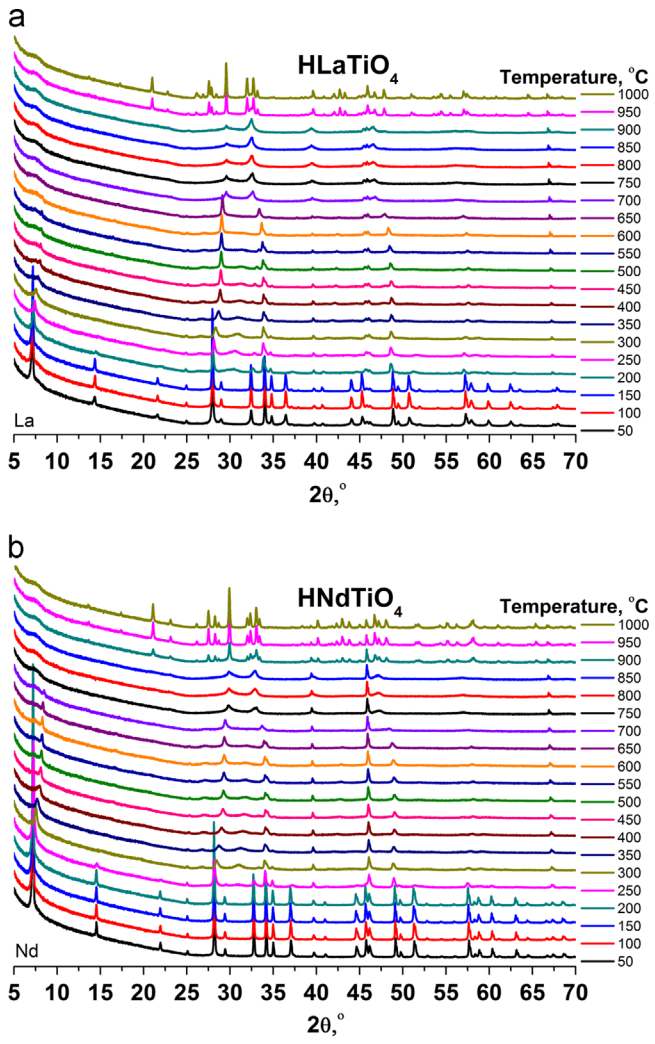

Fig. 2. Thermo XRD data for (a) $HLaTiO_4$ and (b) $HNdTiO_4$ collected from 50 °C to 1000 °C with 50° step.

After the first exothermic transformation and before full water elimination XRD shows the existence of intermediate phases with general formula $Ln_2Ti_2O_7 \cdot xH_2O$. Their structure seems close to defect perovskite $Ln_2{\square}Ti_2O_7$ described previously [29], but with enlarged layer thickness. After full elimination of water (500 °C) XRD detects a single phase – defect perovskite $Ln_2{\square}Ti_2O_7$. Intermediate phases $Ln_2Ti_2O_7 \cdot xH_2O$, as well as fully dehydrated $Ln_2{\square}Ti_2O_7$, can be quite well indexed in primitive tetragonal symmetry. The second exothermic effect (720 °C for La and 760 °C for Nd) corresponds to the structural transformation of defect $Ln_2{\square}Ti_2O_7$ compounds to the $Ln_2Ti_2O_{7\ (p)}$ compounds with pyrochlore structure [33]. The third exothermic effect (990 °C for La and 945 °C for Nd) corresponds to final transformation from pyrochlore phase to the 110 layered perovskite $Ln_2Ti_2O_7$ structure. Titanates with the last type of structure are actively studied as materials for photocatalytic water splitting [34–36]. Table 2 presents the amount of water and structural parameters of samples obtained at different dehydration conditions.

3.3. Transition IR-spectroscopy study

Solid state IR-data of $Ln_2Ti_2O_7 \cdot xH_2O$ samples prepared at different temperatures are presented in Fig. 3.

As it can be seen, both initial H*Ln*TiO_4 samples calcined at 120 °C (Fig. 3, 1) have three-band spectra with some minor splitting typical for cationic ordered layered oxides A*Ln*TiO_4 [37–39]. The band around 400 cm^{-1} can be assigned to the deformational modes of the TiO_6 octahedra, the middle energy band near 600 cm^{-1} corresponds to the equatorial Ti–O stretching, while the high energy band near 800 cm^{-1} can be ascribed to the stretching mode of Ti–O apical bond toward the protonic layer, similar as in Na*Ln*TiO_4 compounds [38], but with significant shift to lower energies. Another low intensity band found near 500 cm^{-1} probably can be characterized as Ti–O apical bond stretching toward the Ln layer. In high frequencies region there exists a wide band corresponding to the hydrogen bonded O–H stretchings in the 2500–3500 cm^{-1} regions. Surface water is presented as enlarged band near 3450 cm^{-1} and band near 1650 cm^{-1}.

IR spectra of partially (Fig. 3, 2–3) and fully dehydrated H*Ln*TiO_4 samples (Figs. 3 and 4) are similar to each other and demonstrate stretching bands shift to the higher frequencies region. High energy band near 800 cm^{-1} corresponding to the apical Ti–O stretchings disappear for totally dehydrated samples while a new band at the higher energies region near 900 cm^{-1} appears most probably belonging to the new linkage between octahedral in structure of defect $Ln_2{\square}Ti_2O_7$ (Fig. 4, c). IR-spectra of partially dehydrated compounds heating up to 250 °C for La-containing oxide and 300 °C for Nd-containing show bands in high frequencies region characteristic for hydrogen bonded O–H groups as well as residual band near 800 cm^{-1} corresponding to Ti–O apical bond

Table 2
Composition of samples obtained after the calcination of $HLaTiO_4$ and $HNdTiO_4$ at different temperatures.

Sample	$HLaTiO_4$					$HNdTiO_4$				
Heating rate 10 °C (min)	*T* (°C)	Time (min)	Composition	*a,b* (Å)	*c* (Å)	*T* (°C)	Time (min)	Composition	*a,b* (Å)	*c* (Å)
	120	30	$HLaTiO_4 \cdot 0.1H_2O$	3.72	12.29	120	30	$HNdTiO_4$	3.69	12.06
	250	1	$La_2Ti_2O_7 \cdot 0.76H_2O$	3.74	24.48	300	1	$Nd_2Ti_2O_7 \cdot 0.71H_2O$	3.70	23.98
	250	30	$La_2Ti_2O_7 \cdot 0.58H_2O$	3.75	23.82	300	30	$Nd_2Ti_2O_7 \cdot 0.34H_2O$	3.70	23.14
	500	30	$La_2Ti_2O_7$	3.75	21.74	500	30	$Nd_2Ti_2O_7$	3.69	21.18

toward the protonic layer. These bands disappear for samples obtained after 30 min heating. In addition XRD patterns of all dehydrated samples did not contain peaks corresponding to the initial protonated H*Ln*TiO_4 compounds. In the case of more hydroscopic La-containing compounds, low intensity bands characteristic for surface water exist for all measured samples. Existence of Ti–O apical bond stretching for samples with high water content $Nd_2Ti_2O_7 \cdot 0.71H_2O$ and $La_2Ti_2O_7 \cdot 0.76H_2O$ suggests that remaining hydrogen exists as part of unmerged titanium–oxygen octahedra (Fig. 4, b).

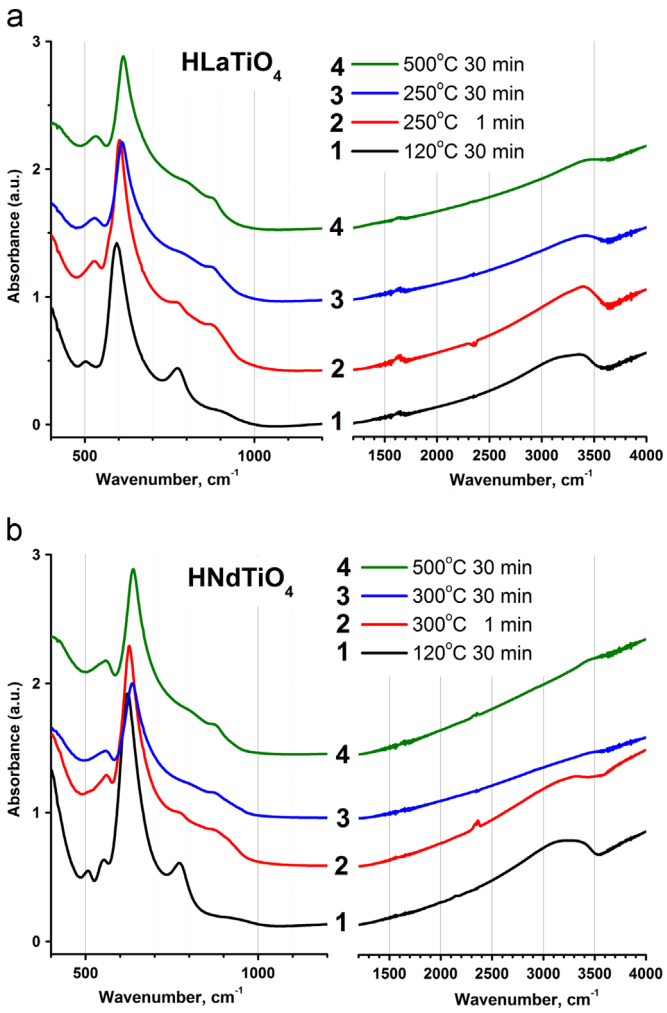

Fig. 3. FTIR spectra of (a) $HLaTiO_4$ and (b) $HLaTiO_4$ after calcination at different temperatures.

3.4. Phase transitions

Possible structural evolutions of H*Ln*TiO_4 compounds during dehydration process and further heating (reactions 1–2) are presented in Fig. 4. The formation of defect structure begins with the formation of new bounds between the axial oxygen and titanium atoms from opposite octahedral layer before the complete elimination of water. The linkage of octahedral layers is accompanied by the shift from eclipsed to staggered conformation (Fig. 4, aand b).

Residual water exists in the form of remaining unmerged octahedra (Fig. 4, b) which during further heating and dehydration link in the defect perovkite structure (Fig. 4, b and c). Low reflections intensity and peak broadening apparently tell about disordering and/or low crystallinity of defect phases. A possible reason could be the migration of some Ln-cations from A-sites of interlayer space to the vacant B-sites of perovskite blocks (Fig. 4, c and d). The similar behavior was observed for some $H_2Ln_2Ti_3O_{10}$ compounds where dehydration accompanies with the movement of some of the Ln^{3+} from the perovskite block to the interlayer gallery stabilizing the layered structure [27]. So here can be a reverse situation driven by high charge difference between perovskite and rock-salt layers. This could explain the observed *c* lattice parameter shrinkage after full dehydration during calcination at high temperature.

Thus the processes occurring during the heating of H*Ln*TiO_4 (*Ln*=La, Nd) can be represented as five main steps:

1. Surface water elimination.
2. Formation of $Sr_3Ti_2O_7$-like structure (Fig. 4, a and b).

$$2HLnTiO_4 \xrightarrow{T} Ln_2Ti_2O_7 \cdot xH_2O. \quad (1)$$

3. Elimination of remaining water, formation of defect $Ln_2{\square}Ti_2O_7$ oxide (Fig. 4, b and c).

$$Ln_2Ti_2O_7 \cdot xH_2O \xrightarrow{T} Ln_2{\square}Ti_2O_7. \quad (2)$$

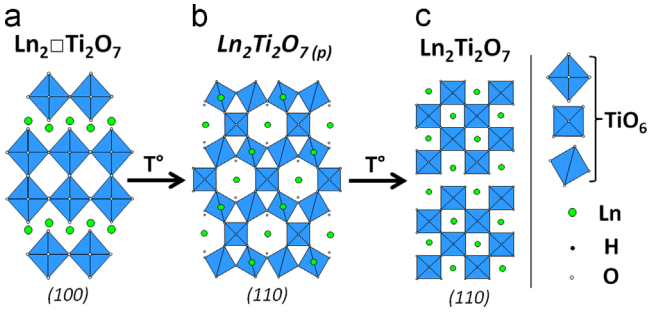

Fig. 5. Structural transformations of $Ln_2{\square}Ti_2O_7$ compounds during heating.

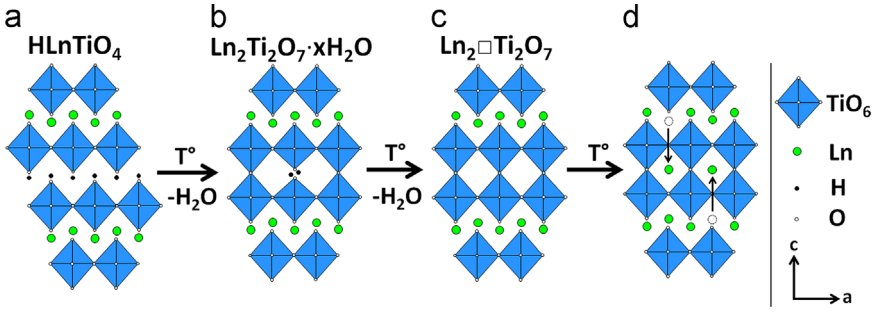

Fig. 4. Structural transformations of H*Ln*TiO_4 compounds during dehydration.

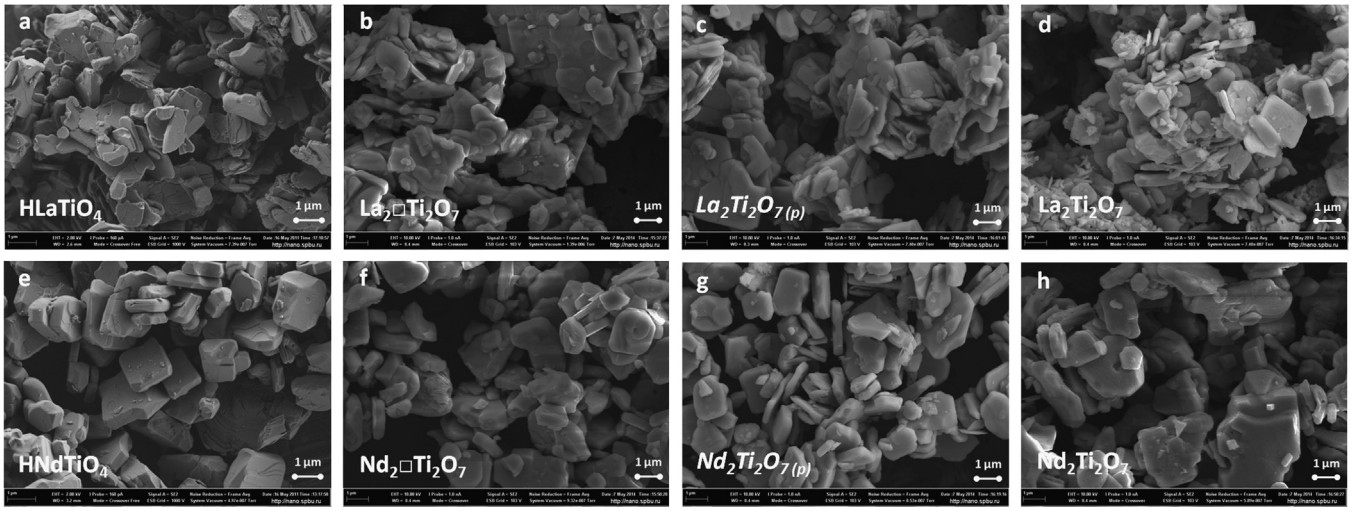

Fig. 6. SEM images of initial protonated layered perovskite-type oxides H*Ln*TiO_4, defect $Ln_2{\square}Ti_2O_7$ oxides, pyrochlore $Ln_2Ti_2O_{7\ (p)}$ oxides, and corresponding 110 layered perovskites $Ln_2Ti_2O_7$ for *Ln*=La (a–d) and Nd (e–h).

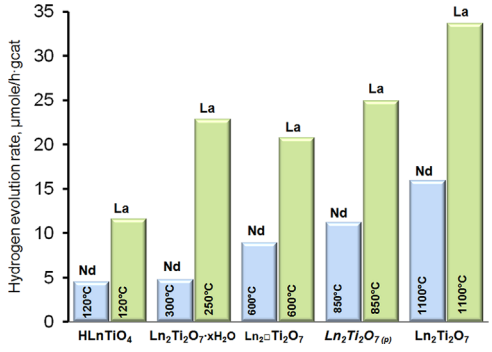

Fig. 7. Photocatalytic activity of investigated samples in the reaction of hydrogen evolution from aqueous isopropanol solution under UV-light irradiation

4. Transformation to pyrochlore phase (Fig. 5, a and b)

$$Ln_2{\square}Ti_2O_7 \xrightarrow{T} Ln_2Ti_2O_{7\ (p)}. \quad (3)$$

5. Transformation to the 110 layered perovskite (Fig. 5, b and c)

$$Ln_2Ti_2O_{7\ (p)} \xrightarrow{T} Ln_2Ti_2O_7. \quad (4)$$

SEM images of samples obtained after heating up to 500 °C ($Ln_2{\square}Ti_2O_7$), 800 °C ($Ln_2Ti_2O_7$) and 1100 °C ($Ln_2{\square}Ti_2O_7$) show that there is no significant change in particles morphology of defect, pyrochlore and layered 110-type perovskite samples compared to initial H*Ln*TiO_4 compounds (Fig. 6). This suggests that dehydration reaction and further phase transitions during thermolysis are topochemical in essence.

The results of photocatalytic experiments of hydrogen evolution from aqueous isopropanol solution under UV-irradiation over investigated samples are presented in Fig. 7.

It can be seen that the hydrogen evolution rate increased with the increase of calcination temperature of complex oxide samples for both La and Nd series under investigation. Only for partially dehydrated $La_2Ti_2O_7 \cdot 0.76H_2O$ sample hydrogen evolution rate is higher than for corresponding $La_2{\square}Ti_2O_7$ compound. The lanthanum-containing compounds were found to be more photocatalytically active, than the corresponding neodymium-containing oxides, which is in good agreement with known data on $Ln_2Ti_2O_7$ photoactivity [36]. The particle morphology of the samples remains almost the same, thus no significant influence of geometrical features like surface area on the photocatalytic activity takes place. This suggests that structural changes occurring during topochemical dehydration of H*Ln*TiO_4, namely, the formation of links between adjacent titanium–oxygen octahedra, play a prominent role for the photocatalytic activity.

4. Conclusions

Thermal dehydration of H*Ln*TiO_4 (*Ln*=La, Nd) compounds as well as further phase transitions during heating were studied. By means of TG, DSC and Thermo-XRD analysis it was found that considered substances form defect layered perovskite-like oxides $Ln_2{\square}Ti_2O_7$ after full dehydration (450–500 °C) while a range of partially dehydrated compounds with general formula $Ln_2Ti_2O_7 \cdot yH_2O$ are formed under lower temperatures. These compounds have a structure close to the layered $Ln_2{\square}Ti_2O_7$ defect oxides but with enlarged lattice parameter. Accordingly to the FTIR data partially dehydrated compounds most likely consist of merged (like in $Ln_2{\square}Ti_2O_7$) and unmerged (like in H*Ln*TiO_4) titanium–oxygen octahedra. Further heating of metastable defect $Ln_2{\square}Ti_2O_7$ substances leads to the phase transition with formation of pyroclor-type oxides $Ln_2Ti_2O_{7\ (p)}$, which in turn transform to stable layered 110-type perovskites $Ln_2Ti_2O_7$ under higher temperatures. The observed phase transformations lead to increase of photocatalytic activity in the reaction of hydrogen evolution from aqueous isopropanol solution.

Acknowledgments

This research was supported by the Russian Foundation for Basic Research (Grant 15-03-05981) and Saint Petersburg State University (Grant 12.38.257.2014). Authors also are grateful to Saint Petersburg State University Research Park. TG and DSC study were carried out in Center of Thermal Analysis and Calorimetry, XRD study was carried out in Research Centre for X-ray Diffraction Studies, IR-study was carried out in Center for chemical analysis and materials research, SEM images were obtained in Interdisciplinary Resource Center for Nanotechnology.

Appendix A. Supplementary information

Supplementary data associated with this article can be found in the online version at http://dx.doi.org/10.1016/j.jssc.2015.02.008.

References

[1] P.M. Shirage, K. Kihou, C.H. Lee, H. Kito, H. Eisaki, A. Iyo, Phys. C Supercond. 484 (2013) 12–15. http://dx.doi.org/10.1016/j.physc.2012.02.039.

[2] H. Asano, J. Hayakawa, M. Matsui, Appl. Phys. Lett. 68 (1996) 3638. http://dx.doi.org/10.1063/1.115755.

[3] A.B. Missyul, I.A. Zvereva, T.T.M. Palstra, A.I. Kurbakov, Mater. Res. Bull. 45 (2010) 546–550. http://dx.doi.org/10.1016/j.materresbull.2010.02.002.

[4] T. Takenaka, H. Nagata, Y. Hiruma, Jpn. J. Appl. Phys. 47 (2008) 3787–3801. http://dx.doi.org/10.1143/JJAP.47.3787.

[5] K. Maeda, J. Photochem. Photobiol. C: Photochem. Rev. 12 (2011) 237–268. http://dx.doi.org/10.1016/j.jphotochemrev.2011.07.001.

[6] I.A. Rodionov, O.I. Silyukov, T.D. Utkina, M.V. Chislov, Y.P. Sokolova, I.A. Zvereva, Russ. J. Gen. Chem. 82 (2012) 1191–1196. http://dx.doi.org/10.1134/S1070363212070018.

[7] I.A. Rodionov, O.I. Silyukov, I.A. Zvereva, Russ. J. Gen. Chem. 82 (2012) 635–638. http://dx.doi.org/10.1134/S1070363212040032.

[8] A. Demont, S. Abanades, E. Beche, J. Phys. Chem. C 118 (2014) 12682–12692. http://dx.doi.org/10.1021/jp5034849.

[9] S. Song, K. Ahn, M.G. Kanatzidis, J.A. Alonso, J.-G. Cheng, J.B. Goodenough, Chem. Mater. 25 (2013) 3852–3857. http://dx.doi.org/10.1021/cm401814z.

[10] K.G.S. Ranmohotti, E. Josepha, J. Choi, J. Zhang, J.B. Wiley, Adv. Mater. 23 (2011) 442–460. http://dx.doi.org/10.1002/adma.201002274.

[11] R.E. Schaak, T.E. Mallouk, Chem. Mater. 14 (2002) 1455–1471. http://dx.doi.org/10.1021/cm010689m.

[12] E.A. Josepha, S. Farooq, C.M. Mitchell, J.B. Wiley, J. Solid State Chem. 216 (2014) 85–90. http://dx.doi.org/10.1016/j.jssc.2014.04.024.

[13] K.G.S. Ranmohotti, M.D. Montasserasadi, J. Choi, Y. Yao, D. Mohanty, E.A. Josepha, et al., Mater. Res. Bull. 47 (2012) 1289–1294. http://dx.doi.org/10.1016/j.materresbull.2012.03.021.

[14] T.C. Ozawa, M. Onoda, N. Iyi, Y. Ebina, T. Sasaki, J. Phys. Chem. C 118 (2014) 1729–1738. http://dx.doi.org/10.1021/jp410522g.

[15] S. Byeon, J.-J. Yoon, S.-O. Lee, J. Solid State Chem. 127 (1996) 119–122. http://dx.doi.org/10.1006/jssc.1996.0364.

[16] I.A. Zvereva, O.I. Silyukov, M.V. Chislov, Russ. J. Gen. Chem. 81 (2011) 1434–1441. http://dx.doi.org/10.1134/S1070363211070061.

[17] O. Silyukov, M. Chislov, A. Burovikhina, T. Utkina, I. Zvereva, J. Therm. Anal. Calorim. 110 (2012) 187–192. http://dx.doi.org/10.1007/s10973-012-2198-5.

[18] V. Thangadurai, A. Shukla, J. Gopalakrishnan, Solid State Ion. 73 (1994) 9–14. http://dx.doi.org/10.1016/0167-2738(94)90258-5.

[19] G. Mangamma, V. Bhat, J. Gopalakrishnan, S. Bhat, Solid State Ion. 58 (1992) 303–309. http://dx.doi.org/10.1016/0167-2738(92)90132-9.

[20] R.E. Schaak, T.E. Mallouk, J. Solid State Chem. 161 (2001) 225–232. http://dx.doi.org/10.1006/jssc.2001.9303.

[21] L.D. Abdulaeva, O.I. Silyukov, Y.V. Petrov, I.A. Zvereva, J. Nanomater. 2013 (2013) 1–8. http://dx.doi.org/10.1155/2013/514781.

[22] L. Abdulaeva, O. Silyukov, I. Zvereva, Y. Petrov, Solid State Phenom. 194 (2012) 213–216. http://dx.doi.org/10.4028/www.scientific.net/SSP.194.213.

[23] M. Tournoux, R. Marchand, L. Brohan, Prog. Solid State Chem. 17 (1986) 33–52. http://dx.doi.org/10.1016/0079-6786(86)90003-8.

[24] R. Marchand, L. Brohan, M. Tournoux, Mater. Res. Bull. 15 (1980) 1129–1133. http://dx.doi.org/10.1016/0025-5408(80)90076-8.

[25] T. Feist, Solid State Ion. 28–30 (1988) 1338–1343. http://dx.doi.org/10.1007/978-1-4757-9649-0_41.

[26] J. Gopalakrishnan, V. Bhat, Inorg. Chem. 26 (1987) 4299–4301. http://dx.doi.org/10.1021/ic00273a001.

[27] M. Richard, L. Brohan, M. Tournoux, J. Solid State Chem. 112 (1994) 345–354. http://dx.doi.org/10.1006/jssc.1994.1315.

[28] M. Richard, L. Brohan, M. Tournoux, Mater. Sci. Forum 152–153 (1994) 245–250. http://dx.doi.org/10.4028/www.scientific.net/MSF.152-153.245.

[29] V. Thangadurai, J. Gopalakrishnan, G.N. Subbanna, Chem. Commun. 29 (1998) 1299–1300. http://dx.doi.org/10.1039/a802644k.

[30] I.A. Zvereva, O.I. Silyukov, A.V. Markelov, A.B. Missyul', M.V. Chislov, I.A. Rodionov, et al., Glass Phys. Chem. 34 (2008) 749–755. http://dx.doi.org/10.1134/S1087659608060126.

[31] I.A. Zvereva, A.M. Sankovich, A.B. Missyul', Russ. J. Gen. Chem. 80 (2010) 1242–1248. http://dx.doi.org/10.1134/S1070363210070042.

[32] I. Zvereva, I. Rodionov, Photocatalytic properties of perovskite-type layered oxides, in: J. Zhang, H. Li (Eds.), Perovskite: Crystallography, Chemistry and Catalytic Performance, Nova Science Publishers, New York, 2013, pp. 181–198.

[33] M.A. Subramanian, G. Aravamudan, G.V. Subba Rao, Prog. Solid State Chem. 15 (1983) 55–143. http://dx.doi.org/10.1016/0079-6786(83)90001-8.

[34] P. Liu, J. Nisar, B. Sa, B. Pathak, R. Ahuja, J. Phys. Chem. C 117 (2013) 13845–13852. http://dx.doi.org/10.1021/jp402971b.

[35] R. Abe, M. Higashi, K. Sayama, Y. Abe, H. Sugihara, J. Phys. Chem. B 110 (2006) 2219–2226. http://dx.doi.org/10.1021/jp0552933.

[36] D.W. Hwang, J.S. Lee, W. Li, S.H. Oh, J. Phys. Chem. B 107 (2003) 4963–4970. http://dx.doi.org/10.1021/jp034229n.

[37] A.E. Lavat, E.J. Baran, J. Braz. Chem. Soc. 17 (2006) 1436–1439. http://dx.doi.org/10.1590/S0103-50532006000700035.

[38] A.E. Lavat, E.J. Baran, J. Alloy. Compd. 419 (2006) 334–336. http://dx.doi.org/10.1016/j.jallcom.2005.10.014.

[39] A.E. Lavat, E.J. Baran, J. Alloy. Compd. 368 (2004) 130–134. http://dx.doi.org/10.1016/j.jallcom.2003.08.071.